PHYSICAL REVIEW B **66**, 241401(R) (2002)

Nanoscale processing by adaptive laser pulses

Petr Král
Department of Chemical Physics, Weizmann Institute of Science, 76100 Rehovot, Israel
(Received 15 October 2002; published 4 December 2002)

We theoretically demonstrate that atomically precise ''nanoscale processing'' can be reproducibly performed by adaptive laser pulses. We present the new approach on the controlled welding of crossed carbon nanotubes, giving various *metastable* junctions of interest. Adaptive laser pulses could be also used in preparation of other hybrid nanostructures.

DOI: 10.1103/PhysRevB.66.241401 PACS number(s): 78.67.−n, 42.62.−b, 61.46.+w, 81.16.−c

Understanding and fully controlling growth, structural modifications, and coalescence of nanoscale materials has a top technological priority. Many excellent examples of such systems can be found among the numerous types of recently discovered nanotubes.[1–3] These unique materials are usually grown under rather poorly understood conditions using plasma,[4] laser[5] and other strongly nonequilibrium processes, where catalytic atoms can activate ''zipping'' of chemical bonds.[6]

Although artificial nanoscale materials resemble biomacromolecules, they do not possess ''inheritable memories'' analogous to DNA, crucial for their exact reproduction. Thus our principal question is, if we can develop effective atomically precise processing methods, that can reproducibly prepare such systems. This goal has been, for example, achieved in a molecular beam growth of superlattices, where nanoscale patterns in one dimension are practically under full control.[7]

It would be especially attractive to achieve a precise control over some advanced structural modifications. An example is coalescent ''welding'' of tubular structures,[8] which could lead in crossed nanotubes[9] to preparation of strong light-weight nets. As just demonstrated experimentally,[10] atomically smooth welded nanotube structures can be induced by irradiation with electrons of MeV energies. Unfortunately, control over this process is so far limited, and thermal healing of the radiation-induced defects[11] is only partial.

It thus becomes very interesting to consider *thermal* welding of nanotubes, driven by an externally applied pressure. Recent simulations[12,13] have revealed that this approach could produce defect-free welded structures, with deep energy minima. On the other hand, practical applications could also largely benefit from a reproducible preparation of various *metastable* atomically precise structures, with shallow energy minima. An example are nanotube junctions with a ''quasicontinuous'' variation of their atomic structures.

Here, we address this challenging task, and explore the possibility of a reproducible welding of nanotubes, by ''adaptive'' laser pulses. A feedback control of ultrashort chirped pulses is already applied in traditional macrowelding of thin films.[14] A precise nanoscale processing could, in principle, be performed by more sophisticated pulses,[15] prepared in *optimal control techniques*,[16] that can selectively break molecular bonds in gases and liquids.[17] Such pulses possess many degrees of freedom in their complex shaping and tuning, with the potential for a storage of ''production informations.''

In Fig. 1, we present a scheme of the controlled welding of crossed nanotubes, realized by their local excitation with adaptive laser pulses. These pulses induce interband electron transitions in a micron-size region, where the hot carriers emit LO phonons. The generated phonons locally decay and heat nanotubes below their melting point ($T_{melt} \approx 4000$ K).[18] Reconstruction of C bonds is thus induced *thermally* in the contact area, where nucleation energies of potential defects are decreased by external pressure. Since the flipped bonds are selected and directed by the configuration of the whole system and the applied pressure, light pulses mostly control the total *extent* of coalescence. The joined region preserve the hexagonal atomic pattern if the tube structures are complementary (armchair/zigzag).

We start the analysis of the welding control with the description of the nanotube excitation by inhomogeneous light intensity $E(x,t)$.[19] From the Fermi's Golden rule we can estimate the electron/hole injection rate, $\dot{n}_{e(h)}(x,t) \propto |E(x,t)|^2$, in the conduction/valence band of the crossed SWNT. Typically, we use the field intensity $E_0 = 5$ MV/cm at frequency $\omega = 10^{15}\ \mathrm{s}^{-1}$, for which we obtain $\dot{n}_{e(h)} \approx 0.3\ \mathrm{ps}^{-1}$ per unit cell, with 40 C atoms for the (10,10) nanotube.[20] This relatively strong excitation could cause variation of the optical coupling, and even lead to a dielectric breakdown of the system. Nevertheless, it should be possible to adapt the light pulses to these conditions in the learning

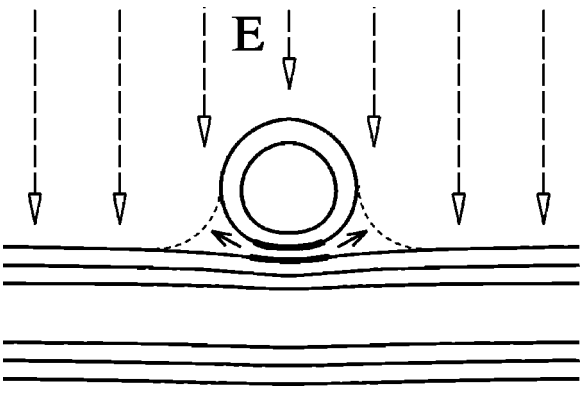

FIG. 1. Coalescent welding of crossed single-wall (SWNT) or multi-wall (MWNT) carbon nanotubes induced by adaptive laser pulses. Local time-dependent excitation heats a micron-size region of the nanotubes, and enables controlled atomically precise restructuralization of C bonds at the pressured tube crossing (thin dashed lines).

process, so the structures could be controllably prepared without destruction.

The hot electrons and holes are generated with energies of a few ($l \approx 3$) LO phonons, which are emitted within $\tau \approx 0.5$ ps. Since the carrier velocity is $v_e \approx 1$ μm/ps, their energy is relaxed within the micron-size generation volume. Therefore, the phonon injection rate $\dot{n}_p(x,t)$ approximately follows the excited electron/hole profile $\dot{n}_p(x,t) \approx l\,[\dot{n}_e(x,t)+\dot{n}_h(x,t)]$. The LO phonons decay locally into LA phonons, which carry most of the heat. Thus the linear density of heat $\mathcal{H}(x,t)$, generated in each of the crossed nanotubes, is of the form

$$\mathcal{H}(x,t) \approx \varepsilon_p\, \dot{n}_p(x,t) \propto 2\, l\, \varepsilon_p |E(x,t)|^2, \tag{1}$$

where $\varepsilon_p = h\nu_0$ is the LO phonon energy.

We can describe the one dimensional transport of heat by the equation

$$S\,\frac{\partial}{\partial x}\left(\kappa(T)\,\frac{\partial T}{\partial x}\right)+\mathcal{H}(x,t)=C(T)\,\rho\,\frac{\partial T}{\partial t}. \tag{2}$$

Here, $\kappa(T)$ is thermal conductivity, $C(T)$ specific heat, $S \approx 1.18$ nm^2 the effective surface per tube in a rope and $\rho = 1.9\cdot 10^{-23}$ kg/nm the mass density of the considered (10,10) armchair nanotube. Both theoretical[21] and experimental[22] results in nanotubes lead to a large $\kappa(T)$, dominated by a phonon transport. From the predicted value $\kappa(T=300\ \mathrm{K}) \approx 7500$ W/K$\cdot$m in SWNT, adjusted to the high-temperature profile in graphite,[23] we obtain $\kappa(T) \approx 23.5\cdot 10^3/T^{1/5}$ W/K$\cdot$m. We can also use the specific heat of graphite,[23] with the high-temperature fit $C(T) \approx 830 + 28.2\,(T-300)^{1/2}$ J/kg$\cdot$K.

The thermally induced coalescence of nanotubes is driven by lessening of the pressure-assisted potential energy of the system (enthalpy), as in sintering. It can be realized by sequences of created and annihilated Stone-Wales (SW) 5/7 defects,[13] and some other types of defects.[10] Typically, the energy of the SW defect is $E_f \approx 2-\epsilon\, C_0$ eV, where ϵ is a local strain.[12] The formation of defects is limited by the size of their activation barrier $E^* \approx 6-\epsilon\, C_0^*$ eV, which can block the process even if $E_f < 0$. The last condition can be met already at strains $\epsilon \approx 0.1$, since $|C_0| \approx |C_0^*| \approx 20$–$30$ eV. Numerical simulations show[12] that the magnitude and sign of the material parameters C_0 and C_0^* depend, in general, on the defect orientation and the tube chirality. Therefore, at the tube crossing, where the pressure-induced strain ϵ is large, only defects with large and negative C_0 and C_0^* would be thermally nucleated.

This fact could significantly reduce the large number of possible coalescence paths, switching between various intermediate structures. The nucleated defects are predominantly chosen by the types of nanotubes, geometry of their crossing and the applied pressure. Therefore, fluctuations of the followed coalescence paths should be relatively small, so that welded structures with the same number of defects could be reasonably *similar*. The most favorable path contains structures with the lowest energies. For example, a head-to-head coalescence of two (10,10) C nanotubes can be realized by following a path with just 68 steps of SW defects.[13] In this process, the flipped bonds first interconnect the tubes, soon after a neck is formed, and finally the tubes become smoothly rejoined (see Fig. 1). The goal of the optimal control is to *deliberately stop* this process at any of the metastable intermediate structures, formed in the vicinity of the most favorable path.

Consider that the system occupies with the probability p_i any of the structures with i defects, formed in the welding process. The probability p_i is described by the rate equation

$$\dot{p}_i = \frac{p_{i-1}}{\tau_{i-1}^+} + \frac{p_{i+1}}{\tau_{i+1}^-} - p_i\left(\frac{1}{\tau_i^+}+\frac{1}{\tau_i^-}\right), \tag{3}$$

where the nucleation time τ_i^+ (τ_i^-) gives the transition rate for creation of $i+1$ ($i-1$) defects, if the system has i defects. The nucleation processes are activated by the temperature at the tube crossing, so the times are

$$(\tau_i^{\pm})^{-1} \approx 2\, N_{at}\, \nu_0\, \exp[-E_{\pm}^*(i)/k_bT]. \tag{4}$$

Here, $N_{at} \approx 20$ is the effective number of C atoms in the local region, $\nu_0 = 10$ ps^{-1} is the vibrational frequency, used also in ε_p, and $E_{\pm}^*(i)$ are activation barriers of the $i+1$th and $i-1$th defects for structures with i defects.

We model these barriers as follows,

$$E_{\pm}^*(i) = 6-\Delta\,\exp[(-|i-j_0|\pm 0.5)/D_i]\ \ \mathrm{eV}, \tag{5}$$

where we assume that the pressure-induced barrier shift, $\Delta > 0$, is exponentially relaxed with the growing number i of defects, since the pressure (motion of the tubes) cannot follow the fast (pulsed) coalescence. In numerical testing, we apply ns welding pulses, separated by μs periods. After the first pulse, the strain ϵ can return to its initial value in all structures, irrespective of their number of created defects j_0. In the next pulse, structures with different number of defects j_0 thus effectively start their evolution with the same barriers $E_{\pm}^*(i=j_0) = 6-\Delta\exp[\pm 0.5/D_i]$. Here, the shifts ± 0.5 reflect the pressure-induced asymmetry in transitions increasing/decreasing the number of defects by one, which is the driving force of the coalescence.

Let us now discuss in more details practical realization of the welding control. In experiments, we can search the optimal field $E(t)$ in a feedback learning loop (see inset of Fig. 4), where we impose our welding requirements. In contrast to the MBE,[7] where growth of individual monolayers is controlled *in situ*, here the light pulses need to be adjusted to the experimentally obtained structures. Mathematically, this search minimizes certain *functional*, which reflects the welding requirements[16] and enables theoretical testing of the method. Since our goal is to reproducibly obtain certain metastable structures, i.e. structures with approximately the same given number $\mathcal{N}_D$ of defects, we look for a field $E(x,t)$ which minimizes the difference

$$F = |\langle \mathcal{N} \rangle - \mathcal{N}_D|, \quad \langle \mathcal{N}^n \rangle = \sum_i p_i i^n. \tag{6}$$

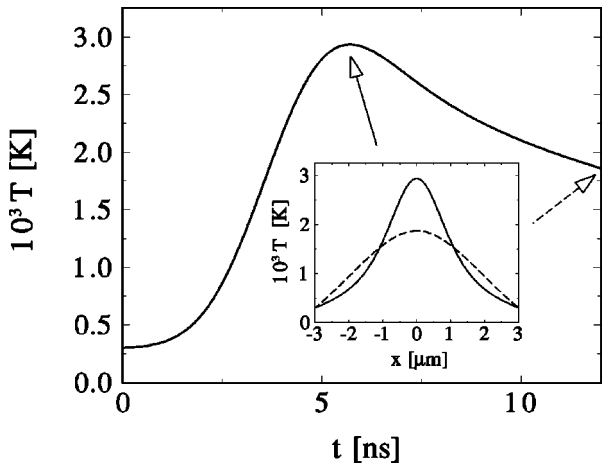

FIG. 2. Time-dependent temperature $T(x,t)$ at the crossing ($x=0$), induced by an optimal pulse. Three such (separated) pulses create in total $\langle \mathcal{N} \rangle \approx 20$ defects. Spatial distributions of $T(x,t)$ at different times are shown in the inset.

Here $\langle \mathcal{N}^n \rangle$ are moments of the distribution p_i. The variance $\sigma_D = \sqrt{\langle \mathcal{N}^2 \rangle - \langle \mathcal{N} \rangle^2}$ describes fluctuations of defects in the prepared structures.

In order to control the nanotube welding, we can take advantage of the fact that the pressure-induced lowering of the barriers $E_{\pm}^{*}(i)$ stops during the *fast* creation of the first D_i defects. Thus, we use short light pulses, heating the system in such a way, that *less* than D_i defects are created by each of them, so that fluctuations in σ_D remain suppressed by the growing barriers $E_{\pm}^{*}(i)$. If we try to induce *more* than D_i defects by a single pulse, then the tubes would have to be largely heated, since the barriers are *not* lowered any more by pressure. Therefore, structural fluctuations would significantly grow and welding could spread without control in the whole region of the crossed tubes. This means that metastable structures with more than D_i defects would have to be prepared by *several* pulses, each generating $\langle \mathcal{N} \rangle < D_i$ defects.

We now test these ideas by solving Eqs. (1)–(6). Since the flipped bonds are largely selected by the system configuration (see above), the field practically only controls the *progress* of welding. Therefore, we can search it in a Gaussian form $E(x,t) = E_0 \exp[-x^2/\sigma_x^2 - (t-t_0)^2/\sigma_t^2]$, where we fix the parameters $\sigma_t = 2.5$ ns ($t_0 = 4$ ns) and $\sigma_x = 1$ μm, and thus choose E_0 as the only varied parameter. In each iteration, of the learning scheme in Fig. 4, we apply three identical (separated) pulses to the system. Then we calculate the difference F, and let E_0 to evolve until F is minimized. In real experiments, we can also vary the *shapes* of the pulses, in order to fit more complex transient conditions.

Here we assume that the nanotubes are in a contact with each other at the crossing and with four contacts (two for each), separated 3 μm away from the tube crossing. They pull the two tubes in opposite directions and thus maintain the vertical force $F = 5-15$ nN [13] at their crossing. We assume that the force leads to the model parameters $\Delta \approx 4$ eV and $D_i \approx 15$, used in Eq. (5). The contacts also provide heat sinks, and are thus held at the temperature $T_0 = 300$ K. In this geometrical configuration, the nanotubes move and restore the force on μs timescale, after each welding pulse.

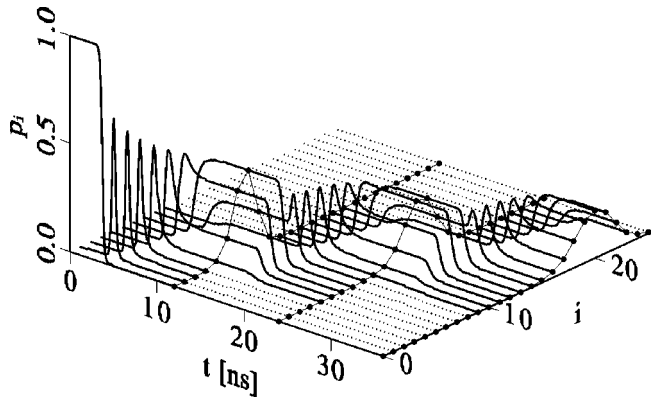

FIG. 3. Time-dependent probabilities $p_i(t)$ of structures with i defects, obtained by excitation with three ns pulses, such as in Fig. 2. The pulses are separated by μs periods, denoted by the dotted lines. With every pulse, the average number of defects moves up, until it reaches $\langle \mathcal{N} \rangle \approx 20$ defects.

Figure 2 shows the temperatures $T(x=0,t)$ at the crossing, induced by excitation with any of the three (separated) laser pulses. By *requesting* that the pulses create in total $\langle \mathcal{N} \rangle \approx 20$ defects, we have obtained their common optimal field amplitude, $E_0 \approx 5$ MV/cm, in several tens of iterations. In the present pulsed regime the temperature rises up to $T \approx 3000$ K, then it slowly relaxes, as the heat diffuses through the tubes, and is pumped out through the contacts. In the inset, we show the related broadening and reshaping of the temperature profile.

In Fig. 3, we show the probabilities $p_i(t)$ of preparing structures with i defects, by application of the above three pulses separated by μs time periods. The pressure-induced coalescence leads to narrow population maxima at certain numbers of defects i after each pulse. The pulse creates less

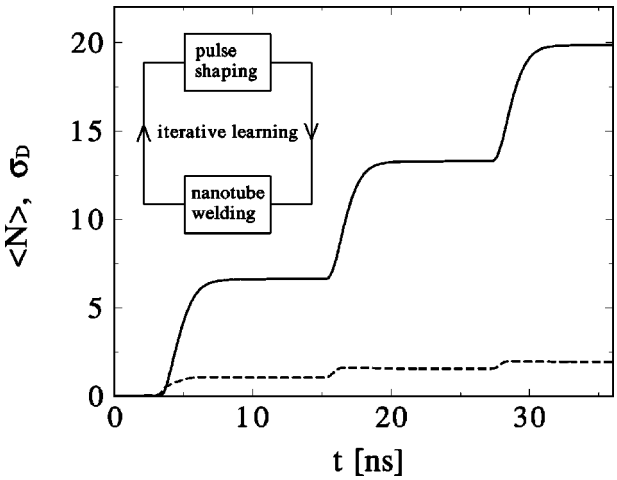

FIG. 4. Time-dependence of the average number of defects $\langle \mathcal{N} \rangle$ (solid line) and their variance σ_D (dashed line) for the pulsed excitation in Fig. 3. In the inset, we show the learning scheme used in optimal control of the welding process.

than D_i defects, before the pressure is temporarily released and the coalescence stops. When the pressure rises again, the process continues with the next pulse, until $\langle \mathcal{N} \rangle \approx 20$ defects are created. In Fig. 4, we also present the time dependence of the average number of defects $\langle \mathcal{N} \rangle$ and the variance σ_D, for the excitation in Fig. 3. The simulation shows that $\langle \mathcal{N} \rangle$ largely depends on the transferred energy, while σ_D remains small, if $\langle \mathcal{N} \rangle < D_1$ within one pulse.

In order to speed up formation of nanotube nets, we can consider simultaneous irradiation of many such junctions under a *mask*, which would concentrate the light on the selected spots. Tubular nets might be also prepared by self-assembly processes, if we succeed to initiate nanotube branching, i.e. splitting of their growth in orthogonal directions.

With more sophisticated light pulses[15–17] the method can also selectively catalyze chemical reactions inside or on the surfaces of nanotubes. This can lead to an efficient preparation of new hybrid materials, with *on-site* grown ''filling'' and ''dressing.'' An example is light-induced polymerization or growth of nanocrystals inside nanotubes.[24] The adaptive pulses could even control electronic processes in nanodevices, especially if the chemical constituents can be reversibly switched by light.[25]

I would like to acknowledge support from EU COCOMO.

[1] S. Iijima, Nature (London) **354**, 56 (1991).
[2] R. Tenne *et al.*, Nature (London) **360**, 444 (1992).
[3] N.G. Chopra *et al.*, Science **269**, 966 (1995).
[4] L.C. Qin, D. Zhou, A.R. Krauss, and D.M. Gruen, Appl. Phys. Lett. **72**, 3437 (1998).
[5] D.B. Geohegan *et al.*, Appl. Phys. Lett. **78**, 3307 (2001).
[6] Y.H. Lee, S.G. Kim, and D. Tománek, Phys. Rev. Lett. **78**, 2393 (1997).
[7] J.A. Roth, W.S. Williamson, D.H. Chow, G.L. Olson, and B. Johs, J. Vac. Sci. Technol. B **18**, 1439 (2000).
[8] P. Nikolaev, A. Thess, A.G. Rinzler, D.T. Colbert, and R.E. Smalley, Chem. Phys. Lett. **266**, 422 (1997); M. Terrones, H. Terrones, F. Banhart, J.-C. Charlier, and P.M. Ajayan, Science **288**, 1226 (2000).
[9] T. Hertel, R.E. Walkup, and P. Avouris, Phys. Rev. B **58**, 13 870 (1998); Y.-G. Yoon, M.S.C. Mazzoni, H.J. Choi, J. Ihm, and S.G. Louie, Phys. Rev. Lett. **86**, 688 (2001).
[10] M. Terrones, F. Banhart, N. Grobert, J.-C. Charlier, H. Terrones, and P.M. Ajayan, Phys. Rev. Lett. **89**, 075505 (2002).
[11] P.M. Ajayan, V. Ravikumar, and J.-C. Charlier, Phys. Rev. Lett. **81**, 1437 (1998); F. Banhart, Rep. Prog. Phys. **62**, 1181 (1999).
[12] G.G. Samsonidze, G.G. Samsonidze, and B.I. Yakobson, Phys. Rev. Lett. **88**, 065501 (2002).
[13] Y. Zhao, B.I. Yakobson, and R.E. Smalley, Phys. Rev. Lett. **88**, 185501 (2002).
[14] F.-R. Tsai and E. Kannatey-Asibu, Jr., J. Manuf. Sci. Eng. **122**, 420 (2000); B.K.A. Ngoi *et al.*, J. Laser Appl. **13**, 41 (2001).
[15] A.M. Weiner and J.P. Heritage, Rev. Phys. Appl. **22**, 1619 (1987); A.M. Weiner, Rev. Sci. Instrum. **71**, 1929 (2000).
[16] D.J. Tannor, R. Kosloff, and S.A. Rice, J. Chem. Phys. **85**, 5805 (1986); A.P. Peirce, M.A. Dahleh, and H. Rabitz, Phys. Rev. A **37**, 4950 (1988).
[17] D. Meshulach and Y. Silberberg, Nature (London) **396**, 239 (1998); T. Brixner, N.H. Damrauer, P. Niklaus, and G. Gerber, Nature (London) **414**, 57 (2001).
[18] H.O. Jeschke, M.E. Garcia, and K.H. Bennemann, Phys. Rev. Lett. **87**, 015003 (2001).
[19] P. Král and J. Mašek, Acta Phys. Pol. A **82**, 697 (1992).
[20] E.J. Mele, P. Král, and D. Tománek, Phys. Rev. B **61**, 7669 (2000).
[21] S. Berber, Y.-K. Kwon, and D. Tománek, Phys. Rev. Lett. **84**, 4613 (2000).
[22] J. Hone, M. Whitney, C. Piskoti, and A. Zettl, Phys. Rev. B **59**, R2514 (1999); J. Hone *et al.*, Appl. Phys. Lett. **77**, 666 (2000).
[23] M. S. Dresselhaus, G. Dresselhaus, K. Sugihara, I. L. Spain, and H. A. Goldberg, *Graphite Fibers and Filaments* (Springer, 1988).
[24] J. Sloan, *et al.*, Chem. Phys. Lett. **329**, 61 (2000).
[25] M. Irie, S. Kobatake, and M. Horichi, Science **291**, 1769 (2001).